

Fuel Effects on Rotating Detonation Engines

Douglas A. Schwer

Kailas Kailasanath

Laboratory for Computational Physics and Fluid Dynamics
Naval Research Laboratory
Washington, DC, USA

1 Introduction

Rotating detonation engines (RDE's) represent a novel approach to using the higher efficiency detonation thermal cycle without some of the drawbacks of pulsed detonation engines (PDE's). Similar to the PDE, the RDE has the advantage of being operated under a wide range of conditions and Mach numbers. Unlike the PDE, it does not have to refill and initiate a detonation 20 to 100 times every second, it provides a steady source of thrust, and can scale up to larger thrust sizes easily, making it an attractive alternative to PDE's. The RDE does have its own set of technical challenges. Since the detonation wave continually runs near the head-end section of the combustion chamber, the inlet micro-nozzles can be subjected to intense pressures and temperatures, and may also be vulnerable to back flow into the premixture plenum. Conditions within the combustion chamber, too, are less well understood than conditions within a PDE, so that designating a combustion chamber to withstand the forces and heat-fluxes typical in an RDE may be more problematic.

The feasibility of RDE's has been experimentally shown at the Lavrentyev Institute of Hydrodynamics [1].

Additionally, there have recently been several numerical investigations into RDE's [2,3]. These studies have focused on an overall description of the flow field within an RDE combustion chamber. We have developed a similar code for simulating two-dimensional and three-dimensional RDE combustion chambers using the same algorithms that have been applied successfully to PDE's and for general detonation research [4-6]. In our previous papers [7,8], we have investigated several different aspects of hydrogen-air RDE's; including pressure effects and engine sizing as well as describing in more detail the features of the flow field.

The present paper extends the current hydrogen-air model to consider various hydrocarbon fuels in both air-breathing mode and rocket mode, and also enables treatment of more complex chemical mechanisms. In particular, we are interested in ethylene-air and propane-air, since both ethylene and propane both have good detonation characteristics and are commonly used in experimental studies of detonation waves and detonation wave engines.

2 Rotating Detonation Engine Model

A basic RDE is shown in Figure 1, with the main features identified in the "unrolled" temperature solution. The combustion chamber is an annular ring, where the mean direction of flow is from the head end (bottom in figure) to the exit plane (top). The micro-nozzles flow in a premixture of fuel and air or oxygen, and a detonation propagates circumferentially around the combustion chamber consuming the freshly injected mixture. The gas then expands azimuthally and axially, and can be either subsonic or supersonic (or both), depending on the back pressure at the outlet plane. The flow has a very strong circumferential aspect due to the detonation wave propagation. Because the radial dimension is typically small compared to the azimuthal and axial dimension, there is generally little variation radially within the flow. Because of this, the RDE is usually "unrolled" into two dimensions, and we will do this for many of our simulations with small thickness to diameter ratios. The main features of an RDE have been discussed previously in our paper [7] and have also been discussed by others [3], typically with the help of temperature and pressure plots of an unrolled RDE simulation.

*. Correspondence to: schwer@lcp.nrl.navy.mil

The current focus of numerical work is on the flow field within an RDE combustion chamber. For the two-dimensional simulations, the azimuthal direction is x , and the axial direction is y . The RDE model follows the Euler model developed in Ref. 7 closely, with some important differences. The conservation equations to be solved are the standard Euler equations, with additional conservation equations for species,

$$\frac{\partial n_i}{\partial t} + \nabla \cdot n_i \mathbf{v} = -\dot{w}_i \quad (1)$$

where the solution variables are density, ρ , velocity, \mathbf{v} , total energy, E , and species concentration, n_i . Pressure is calculated through an equation of state. In previous studies, we used a 2- γ model to calculate the pressure. For this paper, however, we take a different approach that can easily be extended to more complex chemical models. We use 6th order polynomial curve-fits for species enthalpy and the ideal gas law to calculate the pressure P from total energy E and species concentrations n_i :

$$E = \sum_{i=1}^N n_i h_i(T) - P, \quad (2)$$

where $h_i(T) = \sum_{k=0}^K h_{i,k} T^k$ and $h_{i,k}$ are constants for the temperature curve-fit, N is the number of species in the simulation, and K is the order of the polynomial expansion. The system is closed with the ideal gas law,

$$P = \sum_{i=1}^N n_i R_u T \quad (3)$$

where R_u is the universal gas constant. These equations require an iterative solver to determine the pressure given internal energy and species concentrations, however, the system is well behaved and a simple Newton iterator can converge on the correct pressure within 1 or 2 steps usually, and always within 4 or 5 steps.

The reaction rate term, \dot{w}_i , can be calculated through a single or multi-step Arrhenius reaction, or with an induction parameter model [9]. For the induction parameter model, we convect an additional induction variable, τ , with a source term dependent on the induction time:

$$\frac{\partial \tau}{\partial t} + \nabla \cdot \tau \mathbf{v} = \rho / t_{\text{ind}}. \quad (4)$$

In regions where $\tau / \rho > 1$, any reactant is converted to products and heat is released. Care must be taken to spread the heat release out over several time-steps so that the numerical scheme remains stable. Table 1 shows expressions for the induction time used by these models:

Fuel	Expression or model	Comments
Hydrogen	NRL model, table lookup	Kailasanath, K et al, <i>Combust Flame</i> , 61 :3, p 199, 1985.
Ethylene	$t_{\text{ind}} = 3.55 \times 10^{-15} [\text{O}_2]^{-1} \exp(13800/T)$	Hikada, Y et al, <i>Bull Chem Soc Jpn</i> 47 , p 2166, 1974.
Propane	$t_{\text{ind}} = 2.8 \times 10^{-13} [\text{C}_3\text{H}_8]^{0.29} [\text{O}_2]^{-1.19} \exp(18400/T)$	Borisov, AA et al, <i>Proc 9th All-Union Symp on Combust and Explosion</i> , 9 , p 25, 1989.
JP10	$t_{\text{ind}} = 3.47 \times 10^{-15} [\text{JP10}]^{0.67} [\text{O}_2]^{-1.27} \exp(27190/T)$	Davidson, DF et al, <i>Proc Combust Inst</i> , 28 :2, p 1687, 2000.

Table 1. Induction parameter models for various fuels that we use, along with sources.

The boundary conditions are computed assuming small injection nozzles along the head-end face of the combustion chamber. The pressure and temperature for the premixer plenum are set at a constant value; however, the inflow from each nozzle varies considerably depending on where the detonation front is. For the simulation, we do not compute each inlet nozzle, instead we average out the inflow for each computational cell. Conditions that effect the mass flow injection at each cell are the plenum stagnation pressure and temperature (P_{st} and T_{st}), and the combustion chamber pressure, P , in the cell. The boundary con-

ditions at the inlet (P_i, T_i, ρ_i) are computed assuming isentropic expansion through the nozzles into the combustion chamber. The exit boundary condition is a mixed supersonic, subsonic boundary condition, with a small buffer region to damp out reflected waves. Both boundary conditions have been detailed in several papers [7,8], and will not be repeated here.

The solution procedure is based on an FCT-algorithm [10] and domain decomposition for the parallelism. The procedure and convergence criteria has been detailed in previous papers [7]. The simulation has been run using up to 256 cores on a 3 GHz Core 2 Xeon cluster with 8 cores per node and 32 nodes.

3 Detonation Tube Results

Before starting RDE computations, we spent some time with computing detonation waves in tubes to get an idea for how well our numerical models worked on a more standard configuration. The length of the detonation tube is generally 500 mm and is filled with a specified premixture at 300 K, 1 atm. Walls are on either end, and a 1 mm wide driver section is specified at 50 atm and 300 K. The resulting shock wave is typically intense enough to generate a detonation wave, which we can then compare with either CJ properties or other numerical simulations. Typically we used 0.2 mm resolution, however, we have also worked with finer (up to 0.05 mm) and coarser resolutions (0.4 mm), and have found that the global properties do not vary much.

For the majority of our simulations, we considered two-species models for the detonation wave, a reactant and a product specie. The reactant specie is simply a combination of the fuel and air based on the equivalence ratio of the premixture. For this paper, we assume all our simulations are for stoichiometric mixtures. The product species are obtained by running a chemical equilibrium code such as CEA2 [11], and combining the equilibrium species into one product specie. This assumes that in the expansion region, there are no chemical reactions occurring, and thus the product mole fractions will remain constant. For our previous 2- γ models, we compute the value for γ for the reactant at 300 K, and for the product at the CJ temperature, and then scale the heat release so that we reproduce the correct detonation velocity. For this paper, we compute a curve-fit for the reactant and product species based on the actual species curve fits,

$$h_{\text{react},k} = \sum_{i=1}^N X_{i,\text{react}} h_{i,k}, \quad h_{\text{prod},k} = \sum_{i=1}^N X_{i,\text{prod}} h_{i,k}. \quad (5)$$

where $X_{i,\text{react}}$ are the reactant mole-fractions based on stoichiometrics, and $X_{i,\text{prod}}$ are the product mole-fractions based on CEA2 results. We have found that we can accurately reproduce correct pressure and temperature profiles, and detonation wave velocities, with the 2- γ models for a wide-range of fuels and air, and have had considerable success with this model for our hydrogen-air RDE results. A summary of the detonation tube results are shown in Table 2. It is important to note here that we did find it necessary to use curve-fit model for hydrocarbon/air mixtures.

Fuel mixture	W_r	W_p	γ_r	γ_p	$\Delta H_{\text{rxn}}(\text{erg/gm})$	CEA2			LCP-RDE		
						D(m/s)	P(atm)	T(K)	D(m/s)	P(atm)	T(K)
Hydrogen/oxygen	12.0102	14.5028	1.40502	1.21343	8.43×10^{10}	2936	18.77	3676	2836	18.5	3645
Hydrogen/air	20.9114	23.9079	1.40275	1.24259	3.48×10^{10}	1969	15.57	2942	1964	15.5	2930
Ethylene/oxygen	31.0124	22.6717	1.33481	1.23661	5.23×10^{10}	2374	33.42	3934	2382	31.9	3880
Ethylene/air	28.7985	27.9250	1.38116	1.25261	2.85×10^{10}	1824	18.34	2923	1821	18.2	2930
Ethane/oxygen	31.6479	23.7864	1.32503	1.21968	4.87×10^{10}	2247	30.71	3710	2257	29.0	3660
Ethane/air	28.9050	28.0896	1.37912	1.25390	2.485×10^{10}	1710	15.99	2597	1710	15.8	2590
Propane/oxygen	34.0149	22.3919	1.28873	1.22309	5.18×10^{10}	2357	36.17	3824	2354	34.2	3780
Propane/air	29.4654	27.6688	1.36642	1.24999	2.80×10^{10}	1799	18.23	2819	1797	17.5	2790

Table 2. Parameters for 2- γ models and resulting detonation parameters from CEA2 and from the LCP-RDE program. The yellow highlighted mixtures (hydrocarbon-oxygen mixtures) all required curve-fits to reproduce accurate temperature and pressure profiles.

We are also interested in being able to reproduce some of the detonation cellular structure seen in tubes. The first set of detonation structure results are ethylene-air results using the 2-species, induction parameter model discussed above. Traces of maximum pressure results are shown in Figure 2. The domain

length is 1500 mm and the width is 50 mm, with a driver section of 12.5 mm, with a spatial resolution of 0.25 mm x 0.25 mm and time-step of 10^{-8} s. We introduce a 10% perturbation in the pressure in the driver section to give the solution an initial two-dimensionality. It takes about 200 mm before we start to see structure in the maximum pressure, and by 500 mm this structure is seemingly regular, with a width of about 8.3 mm. Further downstream, at about 750 mm, this structure starts to break down, and from there to the end of the tube we no longer see regular structures. Indeed, the detonation seems to have a series of small “explosion” events along a transverse wave, where fuel has built up and suddenly reacts very quickly. A line of these explosive events is mostly clearly seen at about 1300-1350 mm (lowest plot).

4 Rotating Detonation Engine Results

In Figure 3 we show some preliminary results for an RDE running different combinations of ethylene, propane, with both air and oxygen. The geometry is based on previous work [8], with inner and outer diameters of 130 mm and 150 mm, and a length of 177 mm. The back pressure of the combustor is 1 atm, and the plenum stagnation pressure and temperature is 10 atm and 300 K. Both fuels with air are very stable and show almost no instabilities in the slip line between detonated and non-detonated reactants. This is in stark contrast with results with oxygen, which shows very strong instabilities developing along the slip line. All these cases tend to be significantly different from the hydrogen-air calculations run before [7,8]. Table 3 provides a summary of the time-averaged mass flow, force, and fuel based specific impulse calculated from these simulations.

Fuel/Oxidizer Mixture	D_{CJ} (m/s)	Mass flow(kg/s)	Force(N)	Isp(s)
Ethylene/air	1745	1.72	2170	2020
Ethylene/oxygen	2240	1.68	2860	175
Propane/air	1720	1.74	2180	2120
Propane/oxygen	2100	1.75	3020	176
Ethane/air	1630	1.75	2040	2570

Table 3. Performance estimates for the different mixtures. Ethylene and propane have been run both in the rocket mode (using oxygen as the oxidizer) and air-breathing mode (using air as the oxidizer).

5 Summary

We have discussed the extension of our numerical simulations from hydrogen-air RDE’s to hydrocarbon RDE’s. Before beginning the RDE calculations, we have run our models in detonation tubes, and have been able to reproduce CJ temperatures, pressures, and detonation wave velocity found from equilibrium codes such as Gordon and McBride’s. We have also demonstrated the ability to calculate irregular detonation structure using the ethylene-air induction time parameter model. Finally, we have shown some preliminary calculations of hydrocarbon RDE’s running in air and rocket mode. This model appears to provide the right balance between efficiency and complexity to investigate different aspects of hydrocarbon RDE’s, and have shown preliminary results using both air and oxygen for the oxidizer. The overall results for air-breathing RDE’s with hydrocarbons ranged from 2020 to 2570 s, while in rocket mode the specific impulse was around 175 s.

References

1. Bykovskii, F.A., Zhdan, S.A., and Vedernikov, E.F. “Continuous spin detonations,” *JPP* **22**, p 1204, 2006.
2. Zhdan, S.A., Bykovskii, F.A., and Vedernikov, E.F. “Mathematical Modeling of a Rotating Detonation Wave in a Hydrogen-Oxygen Mixture,” *Combustion, Explosion, and Shock Waves* **43**:4, p 449, 2007.
3. Hishida, M., Fujiwara, T., and Wolanski, P. “Fundamentals of rotating detonations,” *Shock Waves*, **19**:1, p. 1, 2009.
4. Kailasanath, K., Oran, E.S., Boris, J.P., and Young, T.R. “Determination of detonation cell size and the role of transverse waves in two-dimensional detonations,” *Combust Flame*, **61**:3, pp 199-209, 1985.

5. Kailasanath, K. and Patnaik, G. "Performance estimates of pulsed detonation engines," *Proc Combust Inst*, **28**, pp 595-601, 2000.
6. Kailasanath, K., Patnaik, G., and Li, C. "On factors controlling the performance of pulsed detonation engines," in *High-speed deflagration and detonation: Fundamentals and control*. Eds: G. Roy, S. Frolov, D. Netzer, and A. Borisov, Moscow, Russia: Enas Publ. 193-206, 2001.
7. Schwer, D.A. and Kailasanath, K. "Numerical Investigation of Rotating Detonation Engines," AIAA Paper 2010-6880, 2010.
8. Schwer, D.A. and Kailasanath, K. "Numerical Investigation of the Physics of Rotating Detonation Engines," *Proc Combust Inst* **33**, in press, 2010.
9. Li, C., Kailasanath, K., and Oran, E.S. "Detonation structure behind oblique shocks," *Phys. Fluids*, **6**:4, pp 1600-1611, 1994.
10. Boris, J.P. and Book, D.L. "Flux Corrected Transport I. SHASTA, A fluid transport algorithm that works," *J Comput Phys*, **11**:3, p 38, 1973.
11. Gordon, S. and McBride, B.J. *Computer Program for Calculation of Complex Chemical Equilibrium Compositions and Applications*, NASA Reference Publication 1311, 1994.

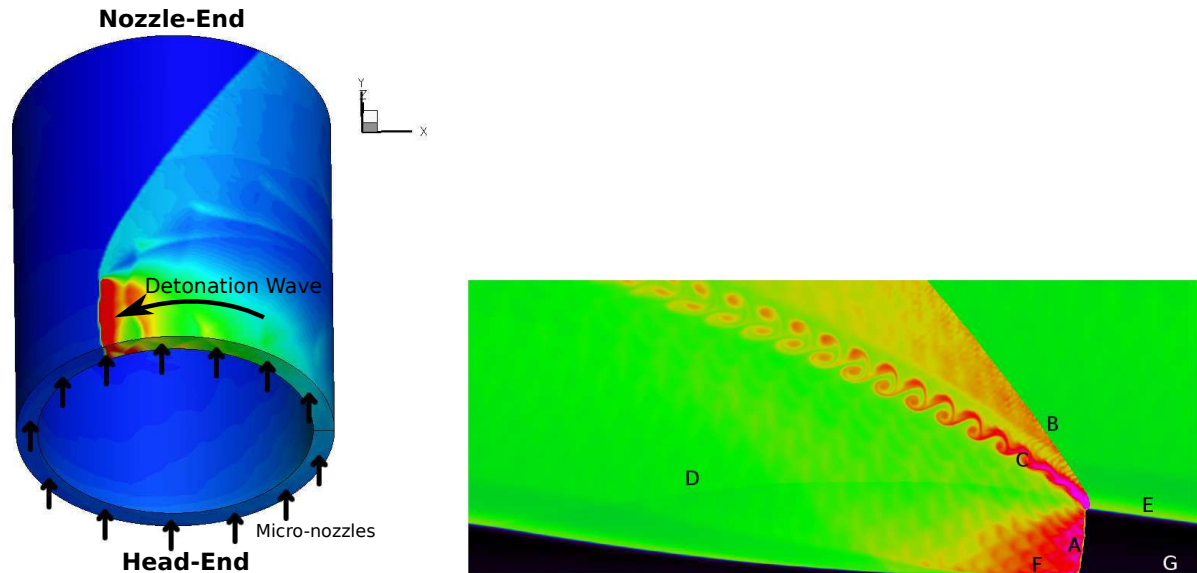


Figure 1. Schematic of three-dimensional RDE showing pressure solution (left) and temperature solution (right) of "unrolled" RDE, where the detonation propagates from left to right. A—detonation wave, B—leading edge shock wave, C—slip line between detonated and non-detonated products, D—expansion region for detonation products, E—non-detonated products from injection and diffusion, F—blocked micro-injectors, G—choked micro-injectors.

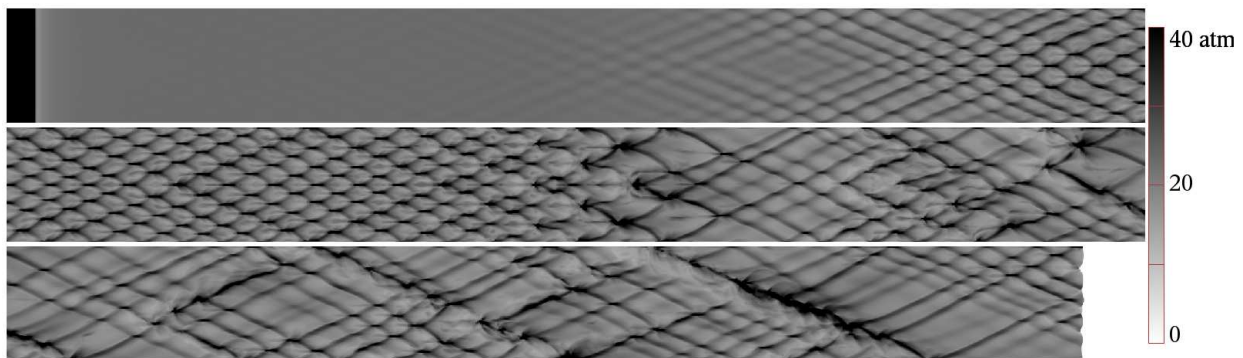


Figure 2. Traces of maximum pressure for ethylene-air flame in a tube. Top plots 0-500 mm, middle is 500-1000 mm, and bottom is 1000-1500 mm and includes the current detonation wave front at about 1460 mm.

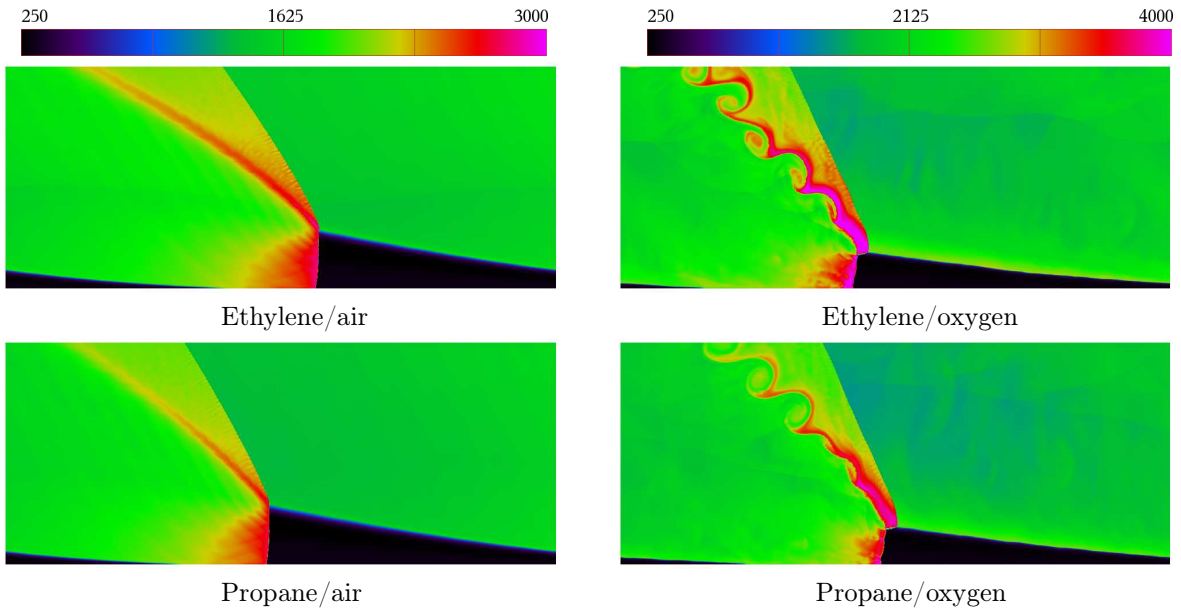


Figure 3. Temperature solution for fuel/air (air-breathing mode) and fuel/oxygen (rocket mode) simulations.